Mode Shape Identification and Orthogonalization

Alvar M. Kabe*
The Aerospace Corporation, El Segundo, California

An identification procedure to improve the mass-weighted orthogonality of measured mode shapes is introduced. The procedure takes into account the degree of mode isolation present during measurement. This is accomplished by establishing a set of new mode shapes, from the measured vectors, that satisfy cross-orthogonality constraints and are a minimum deviation from the measured data. A significant feature is that each measured mode, from which improved modes are identified, can be established using different excitation locations and force levels. This allows the procedure to improve the isolation of modes measured with multishaker sine-dwell testing techniques.

Nomenclature

$[A]_j$ = defined in Eq. (19)
$[B]_j$ = defined in Eq. (19)
$[C]_j$ = defined in Eq. (19)
$\{\bar{C}\}_j$ = defined in Eq. (15)
$[F]$ = excitation force levels
$F_{j\ell}$ = $j\ell$ element of $[F]$
$[G]_j$ = defined in Eq. (19)
$\{G\}_j$ = jth column of $[G]$
$[H]_j$ = defined in Eq. (19)
$\{\bar{I}\}_j$ = defined by Eq. (12)
L = Lagrange function
$[M]$ = mass matrix
$[W]$ = weighting matrix
α_{ij} = defined by Eq. (4)
$[\beta]$ = eigenvalues of $[\phi]^T[M][\phi]$
ζ = critical damping ratio
$[\theta]$ = eigenvectors of $[\phi]^T[M][\phi]$
$[\lambda]$ = matrix of Lagrange multipliers
$\lambda_{\ell i}$ = element of ℓi of $[\lambda]$, Lagrange multiplier
$\{\lambda\}_j$ = jth row of $[\lambda]$
$[\Phi]$ = all the normal modes of a structure
$[\phi]$ = identified mode shapes
$[\bar{\phi}]$ = analytically orthogonalized mode shapes
$[\phi^m]$ = measured modes
$\{\phi\}_j$ = jth column of $[\phi]$
ϕ_{jk} = jk element of $[\phi]$
ϕ^m_{jk} = jk element of $[\phi^m]$
$[\psi]$ = defined by Eq. (17)
$[\Omega]$ = admittance matrix, imaginary components
Ω_{ij} = ij element of $[\Omega]$
$[\bar{\Omega}]_j$ = defined in Eq. (9)
ω_j = frequency of excitation, rad/s
ω_{ni} = ith natural frequency, rad/s
$\odot$ = element-by-element matrix multiplication operator

Introduction

ACCURATE structural dynamic models of complex spacecraft are a requirement. Unfortunately, analytical models agree closely with properly measured mode data only in the first few modes. To minimize the effects of this deficiency, two approaches are used widely. The first approach is to adjust the analytical dynamic model to improve correlation between the analytical and empirical modes. Any remaining difference between the two mode sets is then usually ignored, and the adjusted analytical model is adopted as the model of the actual hardware.

The second approach also involves adjusting the analytical model to improve correlation with the measured modes. However, unlike the first approach, the measured modes are then adopted as the normal coordinates of the dynamic model. This requires that the mode survey test article be representative of flight hardware. The prinipal advantage of this approach is that the influence of deficiencies remaining in the analytical model, after all adjustments have been made, are minimized.

Structural dynamic models of complex space systems typically are formulated by component mode synthesis coupling of substructure modal models. Inherent in the coupling procedures is the assumption that the modes of a substructure are orthogonal with respect to its mass matrix. Therefore, if measured modes are used, any deviation from mass-weighted orthogonality must be corrected.

Numerous procedures have been proposed to orthogonalize measured modes analytically. Gravitz[1] proposed calculating a symmetric influence coefficient matrix by averaging the off-diagonal terms of a matrix obtained from the measured frequencies, measured modes, and the generalized mass matrix. An eigenproblem solution then would yield a set of orthogonal modes. McGrew[2] proposed using the Gram-Schmidt orthogonalization procedure by modifying it to include mass weighting.

Targoff[3] presented a procedure that yielded orthogonal modes by making minimum changes to the measured modes. Subsequently, Baruch and Bar Itzhack[4] demonstrated that Targoff's results could also be obtained by minimizing the mass-weighted difference between the measured and orthogonalized modes. The minimization was performed subject to mass-weighted orthogonality constraints. In Refs. 5 and 6, additional refinements to the procedure of Ref. 4 were introduced. Of particular value is the ability to orthogonalize measured modes relative to each other and to another, already orthogonal set of modes.

An attractive feature of the Ref. 3 procedure, often referred to as the symmetric correction procedure, is that the changes made to the measured data are a minimum. Experience with numerous spacecraft mode sets has demonstrated that if the measured modes satisfy certain orthogonality requirements (i.e., the off-diagonal terms of the unit-normalized, modal mass matrix are less than 0.10), the differences between the measured and orthogonalized modes are small. However, as the modal contamination increases, the required changes obviously become larger. It should be noted that this approach has

Presented as Paper 88-2354 at the AIAA/ASME/ASCE/AHS 29th Structures, Structural Dynamics, and Materials Conference, Williamsburg, VA, April 18-20, 1988; received May 7, 1988; revision received March 23, 1989.

*Manager, Flight Loads Section, Structural Dynamics Department. Member AIAA.

been used successfully in a large number of programs in which the measured modes were used as the normal coordinates of the spacecraft dynamic model.

The Ref. 3 procedure assumes that the lack of orthogonality between any two modes should be corrected by splitting the error equally between the two modes. This approach is adequate for small modal contamination, since the changes thus made are small. This approach is also preferable to other approaches if the contamination is relatively large and the cause of the contamination cannot be established. However, if the cause of the contamination is partly known, before using an approach that arbitrarily splits the error evenly, the known modal contamination should be corrected.

A large number of spacecraft mode survey tests are performed using multishaker, sine-dwell test procedures (e.g., Ref. 7). Frequently, with complex spacecraft, the number of closely spaced modes exceeds the number of available shakers. Under these circumstances, it is often possible to obtain accurate frequency and damping measurements, even though mode shapes of acceptable quality might not be obtained.

If these mode shapes are to be used normal coordinates, they will have to be orthogonalized. However, before using a procedure such as that presented in Ref. 3, it would be advantageous to improve the mode shape orthogonality by considering the degree of isolation that existed when each mode shape was measured. It is the purpose of this paper to introduce an identification procedure that accomplishes the above-mentioned objective.

Theoretical Development

It is reasonable to expect that more accurate mode shapes will result if the degree of mode isolation present during measurement is used to improve the mass-weighted orthogonality of the measured modes prior to analytical orthogonalization. Assume that for each measured mode the natural frequency, critical damping ratio, and shaker force levels and locations are known. In addition, the shaker locations need to be included as degrees of freedom in the measured mode vectors. Furthermore, it will be assumed that any deviation from mass-weighted orthogonality is caused by modal contamination and not errors in the mass matrix.

The mode identification procedure will be derived using constrained minimization theory. To minimize changes to the measured data, the difference between the measured $[\phi^m]$ and identified $[\phi]$ modes will be minimized. Thus, the error function ϵ will be defined as

$$\epsilon = \|[W]([\phi] - [\phi^m])\| = \sum_{i=1}^{n}\sum_{k=1}^{m}\left\{\sum_{j=1}^{n} W_{ij}(\phi_{jk} - \phi_{jk}^m)\right\}^2 \tag{1}$$

where $[W]$ is a square, positive-definite weighting matrix. Note that if $[W] = [M]^{1/2}$, the error function ϵ reduces to the function used in Ref. 4 and would, therefore, be consistent with the orthogonalization procedure of Ref. 3.[4] However, for the derivation presented herein, we shall allow $[W]$ to be any square, positive-definite matrix.

To introduce the degree of isolation that existed when the mode shapes were measured, cross-orthogonality constraints will be imposed on the minimization of Eq. (1). These constraints can be derived from the forced response equation for a linear, elastic structure. By taking advantage of an element-by-element (scalar) multiplication operator $\odot$, described in Ref. 8, the forced response equation can be written as

$$[\phi^m] = [\Phi]\{[\Omega]\odot([\Phi]^T[F])\} \tag{2}$$

where the operations defined in the equation must follow the nesting of the parentheses. Equation (2) is derived in the Appendix.

In Eq. (2), $[\Phi]$ represents all of the mode shapes of the system and, thus, has an infinite number of columns. The matrix $[\phi]$ in Eq. (1) is a column subset of $[\Phi]$. The matrix $[\Omega]$ is the imaginary component of the system admittance matrix, where

$$\Omega_{ij} = \frac{2\zeta_i\alpha_{ij}^3}{[1-\alpha_{ij}^2] + [2\zeta_i\alpha_{ij}]^2} \tag{3}$$

and

$$\alpha_{ij} = \omega_j/\omega_{ni} \tag{4}$$

The columns of $[F]$, which all can be different, are the measured force levels used to establish the corresponding columns of $[\phi^m]$. Therefore, each column of $[\Phi]^T[F]$ represents the modal forces present during measurement of the corresponding columns of $[\phi^m]$. Note that when $[\phi^m]$ is normalized to yield unity on the diagonal of $[\phi^m]^T[M][\phi^m]$, the columns of $[F]$ need to be scaled accordingly.

Premultiplying Eq. (2) by $[\phi]^T[M]$ and taking advantage of the mass-weighted orthogonality exhibited by normal modes, i.e.,

$$\{\phi\}_i^T[M]\{\phi\}_j = 1.0 \quad \text{if} \quad i=j$$
$$= 0.0 \quad \text{if} \quad i\neq j \tag{5}$$

we obtain the cross-orthogonality constraints

$$[\phi]^T[M][\phi^m] = [\Omega]\odot([\phi]^T[F]) \tag{6}$$

The method of Lagrange multipliers[9] will be used to incorporate, in the minimization of ϵ, the constraints defined by Eq. (6). We begin by establishing the Lagrange function L:

$$L = \sum_{i=1}^{n}\sum_{k=1}^{m}\left\{\sum_{j=1}^{n} W_{ij}(\phi_{jk} - \phi_{jk}^m)\right\}^2 + \sum_{\ell=1}^{m}\sum_{i=1}^{m}\lambda_{\ell i}\left(\sum_{j=1}^{n}\sum_{k=1}^{n}\phi_{ji}M_{jk}\phi_{k\ell}^m - \Omega_{it}\sum_{j=1}^{n}\phi_{ji}F_{j\ell}\right) \tag{7}$$

where $\lambda_{\ell i}$ are Lagrange multipliers. Next, we take the partial derivative of L with respect to each of the unknown ϕ_{ij}. These derivatives are set equal to zero to establish a set of $n \times m$ equations that ϕ_{ij} must satisfy for L to be a minimum. Expressing these equations in matrix notation, we obtain

$$2[W]^2([\phi] - [\phi^m]) + [M]^2[\phi^m][\lambda]^T - [F]$$
$$([\Omega]\odot[\lambda])^T = [0] \tag{8}$$

Equations (6) and (8) represent the complete set of equations needed to determine the unknowns $[\phi]$ and $[\lambda]$.

We begin our solution by casting Eq. (6) into a more convenient form. By taking advantage of the element-by-element operator properties,[8] we can write Eq. (2) as

$$[\phi^m] = \sum_{j=1}^{\infty}\{\phi\}_j\{\phi\}_j^T[F][\hat{\Omega}]_j \tag{9}$$

where the elements of the diagonal matrix $[\hat{\Omega}]_j$ are the elements of the jth row of $[\Omega]$, i.e.,

$$\hat{\Omega}_{\ell k} = \Omega_{jk} \quad \text{for} \quad \ell = k$$
$$= 0 \quad \text{for} \quad \ell \neq k$$

Next, we transpose Eq. (9) and postmultiply by $[M][\phi]$ to obtain

$$[\phi^m]^T[M][\phi] = \sum_{j=1}^{\infty}[\hat{\Omega}]_j[F]^T\{\phi\}_j\{\phi\}_j^T[M][\phi] \tag{10}$$

Taking advantage of Eq. (5), we can reduce Eq. (10) to

$$[\phi^m]^T[M][\phi] = \sum_{j=1}^{m} [\hat{\Omega}]_j[F]^T\{\phi\}_j\{\hat{I}\}_j^T \tag{11}$$

where

$$\{\hat{I}\}_j^T = \{\phi\}_j^T[M][\phi] \tag{12}$$

and

$$\hat{I}_{il} = 1 \quad \text{if} \quad i = j$$
$$= 0 \quad \text{if} \quad i \neq j$$

Note that unlike Eq. (9), which involved all of the normal modes of the system, Eq. (11) contains only those modes for which there are measurements. This is consistent with our understanding that the only modes that can be identified are those for which we have data.

Proceeding, we premultiply Eq. (8) by $\frac{1}{2}[W]^{-2}$ and solve for $[\phi]$:

$$[\phi] = [\phi^m] - \tfrac{1}{2}[W]^{-2}[M][\phi^m][\lambda]^T + \tfrac{1}{2}[W]^{-2}$$
$$[F]([\Omega]\odot[\lambda])^T \tag{13}$$

The jth column of $[\phi]$ is, therefore,

$$\{\phi\}_j = [\phi]\{\hat{C}\}_j \tag{14}$$

where

$$\hat{C}_{il} = 1 \quad \text{for} \quad i = j$$
$$= 0 \quad \text{for} \quad i \neq j \tag{15}$$

Substituting Eq. (14) into Eq. (11) yields

$$[\phi^m]^T[M][\phi] - \sum_{j=1}^{m} [\hat{\Omega}][\hat{\Omega}]_j[F]^T[\phi]\{\hat{C}\}_j\{\hat{I}\}_j^T = [0] \tag{16}$$

Equations (16) and (13) now can be used to solve for $[\lambda]$, and then Eq. (13) can be used to obtain the desired modes $[\phi]$.

The product $\{\hat{C}\}_j\{\hat{I}\}_j^T$ in Eq. (16) allows us to solve for $[\lambda]$ one column at a time. Therefore, we can write Eq. (16) as a set of m equations of the form

$$([\phi^m]^T[M] - [\hat{\Omega}]_j[F]^T)[\phi]\{\hat{C}\}_j = \{0\} \qquad j = 1,2,\ldots,m \tag{17}$$

Substituting Eq. (13) into Eq. (17) yields

$$\{[G]_j + [\bar{\lambda}] + [H]_j([\bar{\Omega}]\odot[\bar{\lambda}])\}\{\hat{C}\}_j = \{0\}$$
$$j = 1,2,\ldots,m \tag{18}$$

where

$$[\bar{\Omega}] = [\Omega]^T \qquad [\bar{\lambda}] = [\lambda]^T$$
$$[G]_j = [A]_j^{-1}[C]_j \qquad [H]_j = [A]_j^{-1}[B]_j$$

and

$$[A]_j = -\tfrac{1}{2}\left\{[\phi^m]^T[M] - [\hat{\Omega}]_j[F]^T\right\}[W]^{-2}[M][\phi^m]$$

$$[B]_j = \tfrac{1}{2}\left\{[\phi^m]^T[M][W]^{-2}[F] - [\hat{\Omega}]_j[F]^T[W]^{-2}[F]\right\}$$

$$[C]_j = [\phi^m]^T[M][\phi^m] - [\hat{\Omega}]_j[F]^T[\phi^m]$$

Because of the definition of $\{\hat{C}\}_j$, the jth column inside the braces in Eq. (18) must equal zero. All other columns are arbitrary. Therefore, Eq. (18) reduces to

$$[G]_j + [\bar{\lambda}] + [H]_j([\bar{\Omega}]\odot[\bar{\lambda}]) = [0] \tag{19}$$

Note that the preceding equation can be used to obtain a unique solution for the jth column of $[\bar{\lambda}]$ only. Therefore, to obtain the complete matrix $[\bar{\lambda}]$, Eq. (19) must be solved m times, i.e., $j = 1,2,\ldots,m$.

Because of the element-by-element multiplication operator in Eq. (19), each column of $[\bar{\lambda}]$ can be obtained independently of the other columns, i.e.,

$$\{\bar{\lambda}\}_j = -([I] + [H]_j[\bar{\Omega}]_j)^{-1}\{G\}_j \tag{20}$$

where $\{\bar{\lambda}\}_j = j$th column of $[\bar{\lambda}]$, $\{G\}_j = j$th column of $[G]$, and

$$\bar{\Omega}_{lk} = \bar{\Omega}_{kj} = \Omega_{jk} \quad \text{for} \quad l = k$$
$$= 0 \quad \text{for} \quad l \neq k$$

Once we have solved for the m columns of $[\bar{\lambda}]$, we transpose the resulting matrix and substitute it into Eq. (13) to obtain the identified modes. If the modal contamination is due only to the modes represented in the measured set, orthogonal modes should result. However, if part of the modal contamination is due to modes not in the measured set, then the new, identified modes will not be orthogonal. Nonetheless, they should be an improved representation of the true, normal modes of the system. In this case, which undoubtedly will be the most common, any remaining deviation from orthogonality can be eliminated using the procedure of Ref. 3, i.e.,

$$[\bar{\phi}] = [\phi][\theta][\beta]^{-\frac{1}{2}}[\theta]^T \tag{21}$$

where

$[\bar{\phi}]$ = orthogonal mode shapes

$[\theta]$ = eigenvectors of $[\phi]^T[M][\phi]$

$[\beta]$ = diagonal matrix of eigenvalues corresponding to $[\theta]$

Demonstration of Procedure

The mode shape identification procedure will be demonstrated by numerical simulation of a test problem. The procedure will be used to identify improved mode shapes from contaminated modes. The simulated test modes will be obtained from an analytic test structure subjected to multishaker sine-dwell excitation at its natural frequencies.

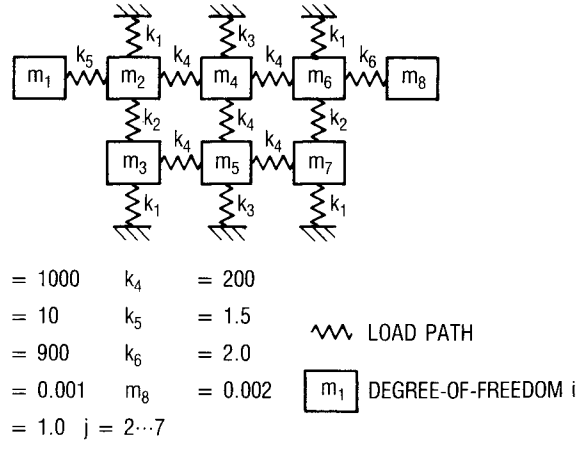

Fig. 1 Analytical test structure.

Table 1 Analytical test structure natural frequencies and modal critical damping ratios

	Mode							
	1	2	3	4	5	6	7	8
f_n, Hz	4.92	5.03	5.26	5.52	5.56	6.16	6.25	6.81
ζ	0.01	0.01	0.015	0.015	0.02	0.01	0.02	0.02

Table 2 Shaker locations and force levels

Shaker location (degree of freedom)	Mode shape							
	1	2	3	4	5	6	7	8
1			4.5	−1.0	−0.45		0.45	
2								
3		1.0	−10.0					
4	1.0			32.0	7.0	28.0	75.0	
5								1.0
6			−4.5	36.0	25.0	−4.0	−3.0	
7				15.0	−15.0			
8								1.0

Table 3 Mass-weighted orthogonality of measured modes

Test Mode	Test Mode							
	1	2	3	4	5	6	7	8
1	1.00	0.27	0.02	0.02	0.01	0.00	0.01	0.00
2		1.00	−0.11	−0.02	0.01	0.00	0.00	−0.12
3			1.00	−0.03	−0.09	−0.05	0.04	−0.05
4				1.00	0.55	0.00	0.00	−0.07
5		SYMMETRIC			1.00	0.02	−0.01	−0.08
6						1.00	0.23	0.03
7							1.00	0.10
8								1.00

Table 4 Mass-weighted orthogonality of first two modes

	Measured modes		Identified modes	
Modes	1	2	1	2
1	1.00	0.27	1.00	0.03
2	0.27	1.00	0.03	1.00

Table 5 Mass-weighted orthogonality of first three modes

	Measured modes			Identified modes		
Modes	1	2	3	1	2	3
1	1.00	0.27	0.02	1.00	0.04	0.00
2	0.27	1.00	−0.11	0.04	1.00	−0.04
3	0.02	−0.11	1.00	0.00	−0.04	1.00

A schematic representation of the analytical test structures is presented in Fig. 1. The springs represent load paths and the squares represent degrees of freedom. The diagonal terms of the diagonal mass matrix and the stiffness values of the load paths are also shown in the figure. The natural frequencies and critical damping ratios for each mode are presented in Table 1.

"Measured" modes were obtained from the closed-form solution for a multidegree-of-freedom system subjected to harmonic excitation. For the test cases, force levels and application points were selected to yield measured modes that were contaminated by modes close in frequency and by modes outside the frequency range of interest. These shaker locations and force levels are presented in Table 2. Note that the excitation levels and locations for each measured mode are distinct. Therefore, the modal forces present when each mode is measured are different. The result of the orthogonality check of the measured modes is presented in Table 3.

To demonstrate the procedure, new modes were identified from the first two, the first three, and the first five measured modes. The identification was also performed using seven measured modes. Table 4 compares the two-mode set, measured-mode, mass-weighted orthogonality to that of the identified modes. As can be observed, the identified modes exhibit considerably better mass-weighted orthogonality than the measured set. In Tables 5 and 6, the measured-mode, mass-weighted orthogonalities for the three- and five-mode sets,

Table 6 Mass-weighted orthogonality of first five modes

	Measured modes					Identified modes				
Modes	1	2	3	4	5	1	2	3	4	5
1	1.00	0.27	0.02	0.02	0.01	1.00	0.03	0.00	0.00	0.00
2		1.00	−0.11	−0.02	0.01		1.00	−0.03	0.00	0.01
3			1.00	−0.03	−0.09			1.00	0.05	−0.03
4		SYMMETRIC		1.00	0.55		SYMMETRIC		1.00	0.31
5					1.00					1.00

Table 7 Comparison of mode shapes

	Measured modes	Identified Modes				Normal modes
		2[a]	3	5	7	
$\{\phi\}_1$	1.03	1.01	1.09	1.08	0.96	0.96
	0.36	0.36	0.35	0.35	0.35	0.35
	0.32	0.34	0.34	0.33	0.32	0.32
	0.44	0.42	0.42	0.42	0.42	0.42
	0.40	0.38	0.38	0.38	0.39	0.39
	0.42	0.42	0.42	0.41	0.41	0.41
	0.33	0.31	0.31	0.33	0.32	0.32
	7.92	8.83	8.83	9.06	9.16	9.18
$\{\phi\}_2$	0.44	0.23	−0.56	−0.41	0.45	0.47
	0.17	0.10	0.12	0.12	0.15	0.16
	0.39	0.24	0.24	0.24	0.24	0.25
	0.20	0.20	0.21	0.21	0.15	0.15
	0.36	0.28	0.27	0.28	0.25	0.25
	0.02	−0.07	−0.06	−0.06	−0.03	−0.03
	0.32	0.26	0.24	0.23	0.23	0.24
	−16.56	−18.57	−18.65	−18.65	−19.02	−19.63
$\{\phi\}_3$	4.53	—	1.67	1.80	1.81	1.84
	0.57	—	0.58	0.49	0.49	0.50
	−0.47	—	−0.46	−0.43	−0.43	−0.43
	0.30	—	0.30	0.31	0.30	0.30
	−0.27	—	−0.27	−0.27	−0.27	−0.28
	0.29	—	0.30	0.39	0.39	0.40
	−0.40	—	−0.40	−0.44	−0.43	−0.44
	−3.77	—	−3.66	−4.23	−4.26	−4.33
$\{\phi\}_4$	−2.79	—	—	−1.18	−2.08	−2.19
	−0.54	—	—	−0.48	−0.41	−0.44
	−0.40	—	—	−0.45	−0.52	−0.55
	0.06	—	—	−0.06	0.02	0.02
	−0.01	—	—	0.04	−0.00	−0.00
	0.64	—	—	0.63	0.45	0.47
	0.33	—	—	0.35	0.49	0.52
	−3.20	—	—	−3.17	−2.22	−2.34
$\{\phi\}_5$	−3.79	—	—	−3.79	−2.63	−2.74
	−0.57	—	—	−0.57	−0.49	−0.51
	0.26	—	—	0.41	0.43	0.45
	0.05	—	—	0.10	0.02	0.02
	−0.02	—	—	−0.04	−0.00	−0.00
	0.67	—	—	0.52	0.52	0.54
	−0.35	—	—	−0.38	−0.46	−0.47
	−3.15	—	—	−2.30	−2.35	−2.44

[a]Number of modes used in identification.

respectively, are compared with the identified modes. As can be ascertained, in each case, the identified modes exhibit improved, mass-weighted orthogonality. The seven-mode case yielded nearly exact modes.

The small, remaining coupling terms are due to imperfect identification. Unless all modes causing contamination are included in the identification, exact correction cannot be achieved. In practice, modes outside the frequency range of interest will not be measured. However, these modes will, to some degree, contaminate the measured set. Therefore, perfect identification should not be expected. Any remaining deviation from ideal mass-weighted orthogonality can then be corrected by a procedure such as in Ref. 3.

In Table 7, the measured and identified mode shapes are compared with the normal modes of the test structure. As the table indicates, the identified modes are in closer agreement with the exact, normal modes than the original measured modes. As expected, the identification becomes more accurate as the number of modes increases. It is encouraging to note that, in general, the degrees of freedom in which the largest changes occurred were those that had the largest errors. More importantly, nearly correct values in the measured modes were altered only slightly.

For the example problems presented herein, the weighting matrix $[W]$ was set equal to $[M]^{1/2}$. As demonstrated in Ref. 4, this weighting is consistent with the assumption made in Ref. 3 of making a minimum change to the measure data. The identifications presented herein were also performed with $[W] = [I]$, i.e., no weighting. However, although dramatic improvements were also obtained, using $[W] = [M]^{1/2}$ yielded superior results. The measured modes were also orthogonalized using the procedure presented in Ref. 3. In each instance, dramatic improvement in the mode shapes was obtained. However, when the procedure presented herein was applied prior to orthogonalization with the Ref. 3 approach, the improvement was always better. This was particularly true for heavily contaminated modes.

Summary

A mode shape identification procedure to improve the isolation of measured modes has been introduced. The procedure was derived by minimizing the difference between the measured and identified modes. The minimization was performed subject to cross-orthogonality constraints, which allow the procedure to take into account the degree of mode isolation present during measurement. A significant feature of the procedure is that each measured mode can be established using different excitation locations and force levels. This allows the procedure to improve the isolation of modes measured with multishaker, sine-dwell test procedures. Another attractive feature is that changes made to the test data are minimal. This paper presents the theoretical formulation and demonstrates the procedure by an example problem.

Appendix

The behavior of a large class of linear, elastic structures subjected to multiple harmonic forces $\{F\}f(t)$ can be described in modal coordinates by

$$[I]\{\ddot{q}(t)\} + [2\zeta\omega_n]\{\dot{q}(t)\} + [\omega_n^2]\{q(t)\} = [\phi]^T\{F\}f(t) \tag{A1}$$

The transformation between physical coordinates $\{x(t)\}$ and modal coordinates $\{q(t)\}$

$$\{x(t)\} = [\phi]\{q(t)\} \tag{A2}$$

and the matrix of mode shape vectors has been normalized with respect to the mass matrix $[M]$ such that

$$[\phi]^T[M][\phi] = [I] \tag{A3}$$

Equation (A1) consists of uncoupled, second-order, differential equations of the form

$$\ddot{q}_i(t) + 2\zeta_i\omega_{ni}\dot{q}_i(t) + \omega_{ni}^2 q_i(t) = \sum_{P=1}^{r} \phi_{Pi}F_P f(t) \tag{A4}$$

where ζ_i and ω_{ni} are the ith mode damping and circular frequency values, respectively, and r is the total number of degrees of freedom in the system. By solving Eq. (A4) for each mode, the acceleration frequency-response function for a typical physical coordinate, x_e, is obtained:

$$\ddot{x}_e(\omega_j)/f(\omega_j) = \sum_{i=1}^{\infty} \left\{ \phi_{ei}(\Omega'_{ij} + \sqrt{-1}\,\Omega_{ij}) \sum_{P=1}^{r} \phi_{Pi}F_P \right\} \tag{A5}$$

where

$$\Omega'_{ij} = -\frac{\alpha_{ij}^2[1-\alpha_{ij}^2]}{[1-\alpha_{ij}^2]^2 + [2\zeta_i\alpha_{ij}]^2} \tag{A6}$$

$$\Omega_{ij} = -\frac{2\zeta_i\alpha_{ij}^3}{[1-\alpha_{ij}^2]^2 + [2\zeta_i\alpha_{ij}]^2} \tag{A7}$$

and

$$\alpha_{ij} = \omega_j/\omega_{ni} \tag{A8}$$

In Eq. (A5), the real part corresponds to the component of acceleration response that is collinear with the reference force, i.e., the coincident (Co) response. The imaginary part corresponds to the component of acceleration response that is 90 deg out of phase with the reference force, i.e., the quadrature (Qd) response. In a multishaker sine-dwell test, the peak quadrature response is used as the measure of mode shape amplitude. Therefore, for the tth mode, the eth degree of freedom measured mode shape amplitude ϕ_{et}^m is given by the imaginary component of $\ddot{x}_e(\omega_t)/f(\omega_{nt})$, i.e.,

$$\phi_{et}^m = \sum_{i=1}^{\infty} \left\{ \phi_{ei}\Omega_{it} \sum_{P=1}^{r} \phi_{Pi}F_{Pt} \right\} \tag{A9}$$

where F_{Pt} is the amplitude of the harmonic force at the pth degree of freedom. The subscript t in F_{Pt} is introduced because the shaker locations and excitation levels can differ for each measured mode.

Equation (A9) can be expanded to all of the degrees of freedom for which measurements are taken, i.e.,

$$\{\phi^m\}_t = [\Phi][\Omega]_t[\Phi]^T\{F\}_t \tag{A10}$$

where

$\{\phi^m\}_t = t$th measured mode

$[\Phi]$ = normal modes of the structure

$[\Omega]_t$ = diagonal matrix, elements defined by Eq. (A7) with

$j = t$

$\{F\}_t$ = shaker force levels used to excite tth mode

We can collect all of the measured modes in a matrix $[\phi^m]$. Since the tth column is given by Eq. (A10), we can write

$$[\phi^m] = [\Phi]\left(\sum_{s=1}^{\infty} [\hat{\Omega}]_s\,[Q]_s\right) \tag{A11}$$

where

$$\hat{\Omega}_{ef} = \Omega_{sf} \quad \text{for} \quad e = s$$

$$= 0 \quad \text{for} \quad e \neq s$$

and

$$Q_{ef} = \{\phi\}_s^T \{F\}_f \quad \text{for} \quad e = f$$
$$= 0 \quad \text{for} \quad e \neq f$$

Equation (A11) can best be explained with a simple example. For a two-degree-of-freedom system, Eq. (A11) would be

$$\begin{bmatrix} \phi_{11}^m & \phi_{12}^m \\ \phi_{21}^m & \phi_{22}^m \end{bmatrix} = \begin{bmatrix} \phi_{11} & \phi_{12} \\ \phi_{21} & \phi_{22} \end{bmatrix} \left(\begin{bmatrix} \Omega_{11} & \Omega_{12} \\ 0 & 0 \end{bmatrix} \begin{bmatrix} \{\phi\}_1^T\{F\}_1 & 0 \\ 0 & \{\phi\}_1^T\{F\}_2 \end{bmatrix} + \begin{bmatrix} 0 & 0 \\ \Omega_{21} & \Omega_{22} \end{bmatrix} \begin{bmatrix} \{\phi\}_2^T\{F\}_1 & 0 \\ 0 & \{\phi\}_2^T\{F\}_2 \end{bmatrix} \right) \tag{A12}$$

$$\begin{bmatrix} \phi_{11}^m & \phi_{12}^m \\ \phi_{21} & \phi_{22}^m \end{bmatrix} = \begin{bmatrix} \phi_{11} & \phi_{12} \\ \phi_{21} & \phi_{22} \end{bmatrix} \begin{bmatrix} \Omega_{11}\{\phi\}_1^T\{F\}_1 & \Omega_{12}\{\phi\}_1^T\{F\}_2 \\ \Omega_{21}\{\phi\}_2^T\{F\}_1 & \Omega_{22}\{\phi\}_2^T\{F\}_2 \end{bmatrix} \tag{A13}$$

$$\begin{bmatrix} \phi_{11}^m & \phi_{12}^m \\ \phi_{21}^m & \phi_{22}^m \end{bmatrix} = \begin{bmatrix} \phi_{11} & \phi_{12} \\ \phi_{21} & \phi_{22} \end{bmatrix} \times \left\{ \begin{bmatrix} \Omega_{11} & \Omega_{12} \\ \Omega_{21} & \Omega_{22} \end{bmatrix} \odot \left(\begin{bmatrix} \phi_{11} & \phi_{12} \\ \phi_{21} & \phi_{22} \end{bmatrix}^T \begin{bmatrix} F_{11} & F_{12} \\ F_{21} & F_{22} \end{bmatrix} \right) \right\} \tag{A14}$$

In Eq. (14), $\odot$ is the element-by-element matrix multiplication operator, and it defines the following operation:

$$[c] = [a] \odot [b] \tag{A15}$$

where

$$c_{ij} = a_{ij} b_{ij}$$

Therefore, using the element-by-element multiplication operator, we can write the matrix of measured modes, $[\phi^m]$, as

$$[\phi^m] = [\Phi]\{[\Omega] \odot ([\Phi]^T[F])\} \tag{A16}$$

and the elements of $[\Omega]$ are defined by Eq. (A7).

References

[1]Gravitz, S. I., "An Analytical Procedure for Orthogonalization of Experimentally Measured Modes," *Journal of Aerospace Science*, Vol. 25, Nov. 1958, pp. 721–722.

[2]McGrew, J., "Orthogonalization of Measured Modes and Calculation of Influence Coefficients," *AIAA Journal*, Vol. 7, April, 1969, pp. 774–776.

[3]Targoff, W. P., "Orthogonality Check and Correction of Measured Modes," *AIAA Journal*, Vol. 14, Feb. 1976, pp. 164–167.

[4]Baruch, M., and Bar Itzhack, I. Y., "Optimal Weighted Orthogonalization of Measured Modes," *AIAA Journal*, Vol. 16, April 1978, pp. 346–351.

[5]Baruch, M., "Selective Optimal Orthogonalization of Measured Modes," *AIAA Journal*, Vol. 17, Jan. 1979, pp. 120–121.

[6]Baruch, M., "Proportional Optimal Orthogonalization of Measured Modes," *AIAA Journal*, Vol. 18, July 1980, pp. 859–861.

[7]Anderson, J. E., "Another Look at Sine-Dwell Mode Testing," *Journal of Guidance, Control, and Dynamics*, Vol. 5, July-Aug. 1982, pp. 358–365.

[8]Kabe, A. M., "Stiffness Matrix Adjustment Using Mode Data," *AIAA Journal*, Vol. 23, Sept. 1985, pp. 1431–1436.

[9]Hadley, G. *Nonlinear and Dynamic Programming*, Addison-Wesley, Reading, MA, 1964.